

Theoretical analysis of the effect of profiled discharge channel on the performance of copper-vapor laser

O.V. Zhdanev and G.S. Evtushenko

Tomsk Polytechnic University
Institute of Atmospheric Optics,
Siberian Branch of the Russian Academy of Sciences, Tomsk

Received December 24, 2002

The effect of a profiled discharge channel on the performance of copper-vapor laser is studied theoretically. The use of a profiled discharge channel leads to an increase of the repetition frequency, power, and performance characteristics of a copper-vapor laser. It is shown that the performance of the copper-vapor laser with the profiled discharge channel is improved due to the increase in radial uniformity of gas temperature and the decrease of the diffusion length.

Introduction

One of the most widely used methods to improve the mean output power of metal vapor lasers is the increase of the pump pulse repetition frequency.^{1,2}

Another possible way of improving the metal vapor laser performance characteristics is to scale a laser active medium of a cylindrical configuration at longitudinal repetitively pulsed discharge.^{1,2} The best results on the mean specific output power are now obtained in small-volume gas-discharge tubes (GDT) (Fig. 1).^{3,4}

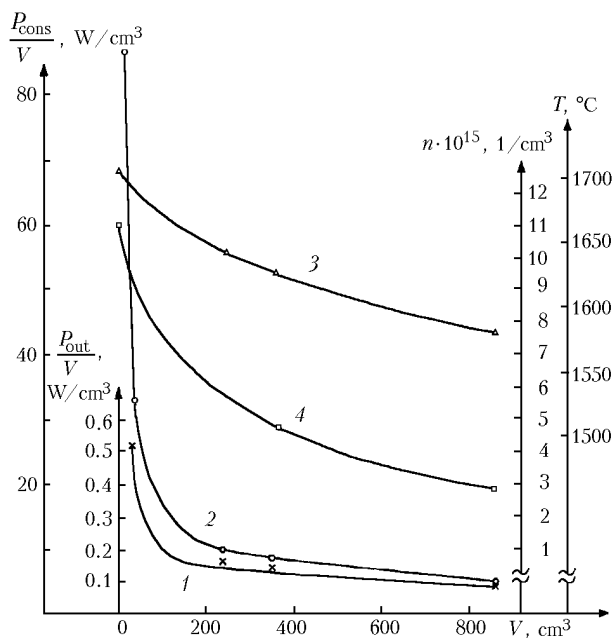


Fig. 1. Specific power consumed by an active element (1), its specific output energy (2), discharge channel temperature (3), and concentration of copper atoms (4) as functions of the volume of active medium.

These parameters were obtained at relatively high pump pulse repetition frequencies.⁵⁻⁷ At the

same time, the best results on practical efficiency were obtained in large-diameter GDT^{8,9} at low pump pulse repetition frequencies and low specific energy depositions of about 1.5–0.5 W/cm³ for GDTs of 6–12 cm in diameter. As the specific energy deposition increases above some value, both the specific emitted energy and the specific output power decrease. This is accompanied by the appearance of significant radial inhomogeneity in the output power. Radially inhomogeneous overheating of the active medium leading to considerable deficit of working element atoms on the GDT axis is one of the most significant factors restricting the increase of laser performance characteristics with the increasing energy deposition.

The investigations performed (Fig. 1 and Refs. 3 and 4) showed that there is a close correlation between the copper vapor concentration and specific emitted power. Thus, to achieve high performance of metal vapor lasers with large volume of the active medium, it is necessary to develop such a design that provides the working temperature of the discharge channel without overheating.

One of the possible ways to designing such a construction is the use of a profiled discharge channel through using radial inserts. By the beginning of this study, there were the following opinions on the mechanisms of influence of radial inserts on copper-vapor laser performance.

A design of a copper-vapor laser (CVL) with a baffle inserted in the discharge channel is described in Ref. 10. The effect of the radial insert is associated in Ref. 10 with two factors:

1. Decrease of the electron temperature leading to the decrease of the pre-pulse concentration of copper atoms in the metastable state;
2. Increase of the discharge resistance, which should lead to better matching with the discharge channel.

The increase of the discharge resistance in Ref. 10 is explained by the increase of the frequency of electron-atom collisions and the decrease of the equilibrium concentration of electrons: $\rho = 1/\sigma = mv/e^2 n_e$, where m is the electron mass; e is the

electron charge; n_e is the electron concentration; ν is the effective frequency of electron collisions. However, Ref. 10 gives no explanations relating the presence of a radial insert in the working channel and the described changes in the plasma parameters. Besides, the use of the active element design proposed in Ref. 10 leads to the radial inhomogeneity of the gas temperature because of anisotropy of the insert design and, as a consequence, to radial non-uniformity of the plasma parameters: temperature and concentration of electrons and copper concentration, causing the decrease of both the output energy and the output beam quality.

From the literature we know the GDT design with a set of coaxially arranged cylindrical thermal screens.^{11,12} However, using this design, Soldatov, Polunin, and Chausova¹² succeeded in providing for the conditions for initiation and maintenance of cross homogeneous discharge only at low buffer gas (neon) pressure $p_{Ne} = 4$ Torr.

To eliminate these disadvantages and obtain high-frequency pumping of a metal vapor laser with an active element of large volume, a GDT design with radial 22XC ceramic inserts with a developed surface (Fig. 2) was proposed.¹³

The use of the radial insert resulted in stable operation at far higher specific and total energy depositions than for the copper-vapor laser with GDT of an ordinary cylindrical design.

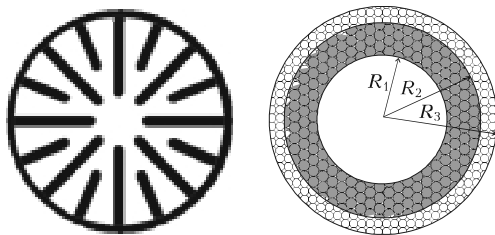


Fig. 2. Schematic profile of the actual GDT (a) and GDT used in calculation of the thermal field (b).

Discharge plasma in metal vapor is characterized by a lot of significantly nonstationary physical parameters and is very difficult for optimization, since changes of the pump parameters (pulse repetition frequency, voltage, current) are strictly restricted by thermophysical properties of the laser cavities. In particular, at high-energy depositions it is necessary, because of the low thermal conductivity of the buffer gas, to provide for additional heat abstraction from the central part of the working channel. The developed active element provide for such capabilities.

This paper presents theoretical analysis of the effect of radial inserts on the performance parameters of copper-vapor laser.

Calculation of temperature field of an active element

The gas temperature of the gas discharge tube is one of the most significant parameters of copper vapor laser plasma, affecting the energy and frequency characteristics. It is not always possible to measure the gas temperature in a wide range of experimental conditions. In this situation, as well as for interpretation of the experimental data available, it is good to apply numerical calculations of the temperature field in GDT. The maximum gas temperature in GDT can be estimated on the assumption that all the energy received by electrons during pumping is transferred to gas particles.¹⁴ In Refs. 13, 14 it was shown that the gas temperature distribution is radially inhomogeneous in self-heating lasers with longitudinal excitation of the active medium, and this distribution corresponds to inhomogeneous energy deposition to the discharge, while the pump energy efflux to GDT walls due to radiation and electron diffusion is neglected. In the case of relatively short GDT (when the ratio of the tube length to its diameter is less than 40–50), the energy loss by radiation should be necessarily taken into account.¹²

In calculating the radial temperature field, as in Ref. 15, three model distributions of the specific energy deposition were used:

1. Uniform distribution $Q_1(r) = P_0$, the energy deposition on the GDT axis $Q_1(0) = P_0$;

2. Parabolic distribution

$$Q_2(r) = 2P_0 (1 - r^2/R_d^2),$$

the energy deposition on the GDT axis $Q_2(0) = 2P_0$, R_d is the inner radius of GDT;

3. Triangular distribution

$$Q_3(r) = 3P_0 (1 - r/R_d),$$

the energy deposition on the GDT axis $Q_3(0) = 3P_0$.

With P_0 unchanged for all the energy depositions, the rate of pump energy input is the same

$$P_{ni} = 2\pi \int_0^{R_d} Q_i(r) r dr.$$

Thermophysical data on alumina 22XC and BeO ceramics and neon buffer gas are borrowed from Refs. 17–19 and given in Table 1.

Table 1. Thermophysical data on alumina 22XC and BeO ceramics and neon buffer gas

Parameter	Neon buffer gas	22XC ceramics	BeO ceramics
Density, kg/m ³	$7.2 \cdot 10^{-3}$	3780	3010
Heat conductivity, W/m·K	$8.96 \cdot 10^{-4} \cdot T_g^{0.683}$	32	15
Heat capacity, J/kg·K	1030	1080	2080
Specific heat	7.42	$4.0824 \cdot 10^6$	$6.2608 \cdot 10^6$
Temperature conductivity (for 1500 K)	$2.6539 \cdot 10^{-7}$	$7.8385 \cdot 10^{-6}$	$2.3958 \cdot 10^{-6}$

The radial temperature distribution of a gas being in a limited volume is established by means of transfer of energy released in discharge through a multicomponent gas medium to walls of the radial insert, then through ceramics to the GDT wall, and then through the wall to the ambient space. In the repetitively pulsed discharge, the gas temperature changes cyclically, increasing during the pump pulse and decreasing in the afterglow. If the following condition is fulfilled^{20,21} the gas cooling time is

$$\tau_{\text{cool}} \cong \frac{pR_{\text{DT}}^2}{6AT_g^{1.683}} \gg \frac{1}{f},$$

where R_{DT} is the outer tube radius of GDT; p is the buffer gas pressure; f is the pulse repetition rate,

$$A = 2.7 \cdot 10^{-2} \frac{\text{cm}^2 \cdot \text{Torr}}{\text{s} \cdot \text{K}^{1.683}},$$

then it can be taken that the gas temperature pulsations are low with respect to the mean temperature. Thus, in considering the high-frequency CVL operation, the thermal problem for such a system can be solved by reducing it to the problem of stationary thermal conditions in an equivalent system of nested cylinders with the first- and third-kind boundary conditions (Fig. 2).

Since the coefficients of temperature conductivity for ceramics are ten times higher than that of the buffer gas, the initial problem can be divided into three ones. The first and the second problems consist in seeking stationary temperature field in 22XC and BeO ceramics, respectively, at constant heat flux to internal surfaces. For the radial insert, the heat flux is equal to the mean input power per unit GDT length with the first-kind boundary conditions on its surface. In this case, for calculation of the temperature field of the GDT wall we know the temperature of the insert surface and the third-kind boundary conditions on the outer side of GDT. The third problem is determination of the stationary temperature field of the cylinder filled with neon buffer gas with the first-kind boundary conditions at the surface temperature determined by the solution of problem 1.

Mathematical formulation of the problem

1. For zone 1 ($r < R_1$)

The thermal conductivity equation in cylindrical coordinates for the first zone is²²:

$$\frac{1}{r} \frac{\partial}{\partial r} \left(\lambda_1(r) r \frac{\partial T_1(r)}{\partial r} \right) = -Q(r).$$

The boundary conditions are:

$$\frac{dT_1(0)}{dr} = 0 \text{ and } T_1(R_1) = T_2(R_1),$$

and

$$\lambda_1(r) = \alpha T^\beta(r),$$

where $Q(r)$ is the specific energy deposition in the discharge; λ_1 is the heat conductivity coefficient of the buffer gas, $\alpha = 8.96 \cdot 10^{-6} T_g^{0.683}$, (W/cm·K), $\beta = 0.683$, $T_1(r)$ is the radial function of the gas temperature in zone 1.

2. For zone 2 ($R_1 < r < R_2$):

$$\frac{1}{r} \frac{\partial}{\partial r} \left(\lambda_2 r \frac{\partial T_2(r)}{\partial r} \right) = 0.$$

Boundary conditions are:

$$\lambda_2 \frac{dT_2(R_1)}{dr} = -P_i \text{ and } T_1(R_1) = T_2(R_1),$$

and

$$\lambda_2 = \frac{S_1 \lambda_1 + S_2 \lambda_2'}{S},$$

S_1 is the cross section area of GDT working channel occupied by the radial insert; S_2 is the cross section area of GDT working channel free of the radial inserts; S is the cross section area of GDT working channel, λ_2' is the heat conductivity coefficient of ceramics.

3. For zone 3 ($R_2 < r < R_{\text{DT}}$):

$$\frac{1}{r} \frac{\partial}{\partial r} \left(\lambda_3 r \frac{\partial T_3(r)}{\partial r} \right) = 0.$$

Boundary conditions are:

$$\lambda_3 \frac{dT_3(R_{\text{DT}})}{dr} - \varepsilon(T_{\text{wall}} - T(R_{\text{DT}})) = 0,$$

(that means that it is assumed that the convective heat exchange between the GDT surface and the ambient medium obeys the Newton–Richman's law^{23,24}) and

$$T_3(R_{\text{DT}}) = T_{\text{wall}},$$

where λ_3 is the heat conductivity coefficient of alumina ceramics^{17,18}; $T_3(r)$ is the function of gas temperature in zone 3; T_{wall} is the temperature of the GDT wall; ε is the heat transfer coefficient.

Solutions of the thermal conductivity equation for the zone ($r < R_1$) corresponding to the model distributions of the energy deposition have the following forms:

1. For the uniform distribution:

$$T_1(r) = \left[T_2(R_1)^{\beta+1} + (R_1^2 - r^2) P_0 \frac{\beta+1}{4\alpha} \right]^{\frac{1}{\beta+1}};$$

2. For the parabolic distribution:

$$T_1(r) = \left[T_2(R_1)^{\beta+1} + (R_1^2 - r^2) P_0 \frac{(\beta+1)}{2\alpha} + \left(\frac{r^4}{R_1^2} - R_1^2 \right) P_0 \frac{(\beta+1)}{8\alpha} \right]^{\frac{1}{\beta+1}};$$

3. For the triangular distribution:

$$T_1(r) = \left[T_2(R_1)^{\beta+1} + (R_1^2 - r^2) P_0 \frac{3(\beta+1)}{4\alpha} + \left(\frac{r^3}{R_1} - R_1^2 \right) P_0 \frac{(\beta+1)}{3\alpha} \right]^{\frac{1}{\beta+1}}$$

For the zone ($R_1 < r < R_2$) the solution for all the distributions has the form

$$T_2(r) = T_3(R_2) + \frac{P_n R_1}{\lambda_2} \ln\left(\frac{R_2}{r}\right).$$

For the zone ($R_2 < r < R_{DT}$) the solution for all the three cases can be represented as follows:

$$T_3(r) = T_{wall} + \frac{P_n R_2}{\epsilon R_{DT}} + \frac{P_n R_2}{\lambda_3} \ln\left(\frac{R_{DT}}{r}\right).$$

The gas temperature average over the GDT cross section was calculated by the following equation¹⁵:

$$\bar{T} = R_1^2 / 2 \int_0^{R_1} \frac{r}{T(r)} dr.$$

The concentration of copper atoms balanced with the temperature of the GDT wall in the range from 1500 to 2000 K can be calculated as follows^{25,26}:

$$\log_{10} N_{Cu} = (0.4477 T_{wall}^{0.7261} - 0.03698 T_{wall} - 15.549) m^{-3}.$$

The radial distribution of the concentration of copper atoms in the ground state was calculated in accordance with the radial distribution of the gas temperature for GDT parameters given in Table 2.

Table 2. GDT parameters

Parameters	GDT with profiled discharge channel	GDT with cylindrical discharge channel
Energy release radius	1.5 cm	2.75 cm
Radial insert thickness	1.25 cm	0
Working channel wall thickness	0.25 cm	0.25 cm

Figure 3a depicts the mean gas temperature in the working channel for GDT with a cylindrical geometry and profiled surface as a function of the specific energy deposition. The plots are drawn depending just on the specific input power, rather than the rate of input power, since GDT with the profiled working channel has different energy release area. It is seen from Fig. 3a that for both types of GDT the increase of the energy deposition leads to a fast increase of the mean gas temperature. However, there is a difference in behavior of the population of the ground level of the copper atom on the GDT axis depending on the specific energy deposition for different geometry of the working channel (Fig. 3b).

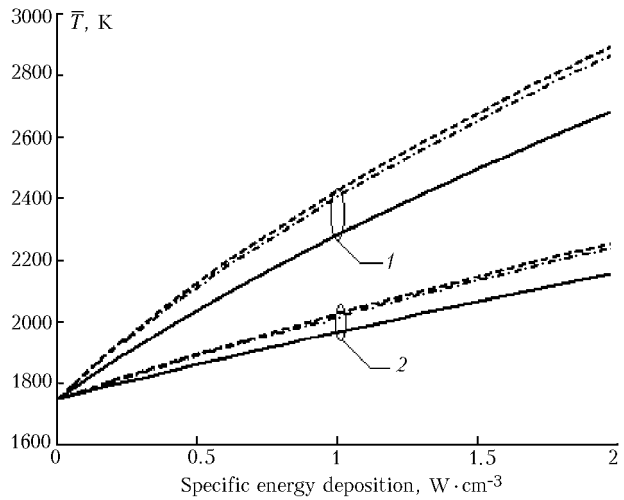


Fig. 3a. Dependence of the gas temperature average over the GDT radius: for cylindrical geometry (1) and for profiled working channel (2); for energy deposition uniform over the cross section of the working channel (solid curve), for triangular distribution of energy deposition (dashed curve), and for parabolic distribution of the energy deposition (dot-and-dash curve).

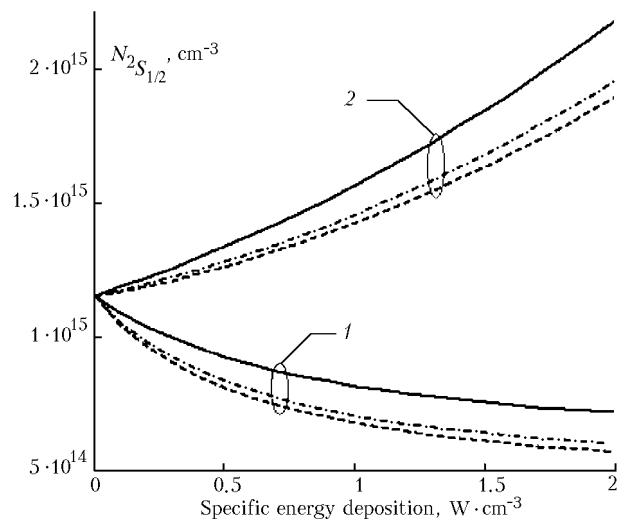


Fig. 3b. Concentration of copper atoms in the ground state on the GDT axis: for cylindrical geometry (1) and for profiled working channel (2); for energy deposition uniform over the cross section of the working channel (solid curve), for triangular distribution of energy deposition (dashed curve), and for parabolic distribution of energy deposition (dot-and-dash curve).

At the standard cylindrical geometry, we can see that the concentration of copper atoms in the ground state $S_{1/2}$ decreases with the increasing specific energy deposition, while for the GDT with the profiled working channel the dependence is quite opposite: the concentration of copper atoms in the ground state increases with the increase of the energy deposited in unit volume. This occurs because, as can be seen from Fig. 3d, the concentration of copper atoms in the laser active medium increases with the increasing specific energy deposition for GDT with

the profiled working channel much faster as compared to GDT of cylindrical design.

As this takes place, the gas temperature on the axis of cylindrical GDT increases faster with the increasing energy deposition than for GDT with the profiled working channel, that is, the temperature on the GDT axis increases faster for the case of the cylindrical working channel (Fig. 3c). Therefore the balanced population of metastable levels of the copper atom is higher in the cylindrical GDT (Fig. 3e).

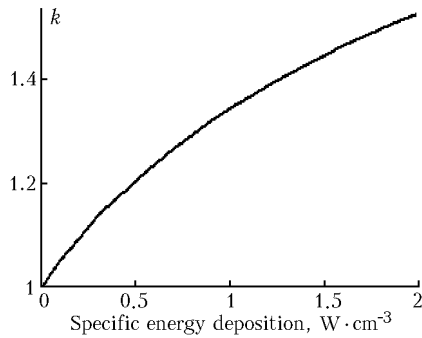


Fig. 3c. Ratio of the temperature on the GDT axis for the case of cylindrical GDT to the temperature on the GDT axis for GDT with profiled working channel.

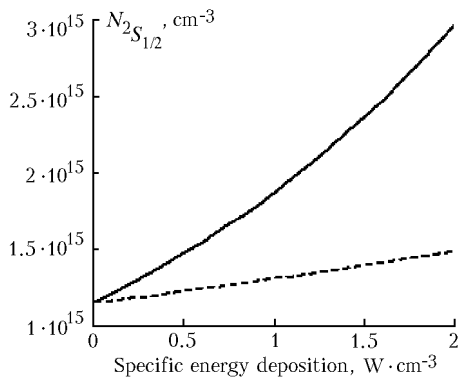


Fig. 3d. Concentration of copper atoms in laser active medium balanced with the temperature of the GDT wall as a function of specific energy deposition; GDT of cylindrical geometry (solid curve) and GDT with profiled working channel (dashed curve).

The radial distributions of the gas temperature in the working channel and concentration of copper atoms in the ground state are depicted in Figs. 4a, and b. It can be seen that for a GDT with the profiled channel the degree of inhomogeneity of the concentration of copper atoms in the ground state is much lower as compared to GDT of cylindrical geometry.

At the deposited power of 1 W/cm³, the ratio of the concentration of copper atoms in the state S_{1/2} balanced with the wall temperature to the concentration of copper atoms on the axis for the cylindrical geometry of the discharge channel is equal to 1.613, while for the profiled discharge channel it is only 1.197, that is, 1.348 times lower. As the specific energy deposition increases, this ratio increases too. Besides, the degree of uniformity in the

distribution of buffer gas atoms over the GDT cross section increases, thus leading to the increase in the frequency of electron-atom collisions (confirming almost completely the point of view proposed in Ref. 10), except for the earliest periods of discharge development that determine the plasma conductivity. This leads to better matching of the active element with the discharge circuit and to an increase in the operation efficiency. Thus, the design of the active element with the profiled discharge channel that was proposed in Ref. 13 is capable of generating more uniform radial distribution of metal vapor.

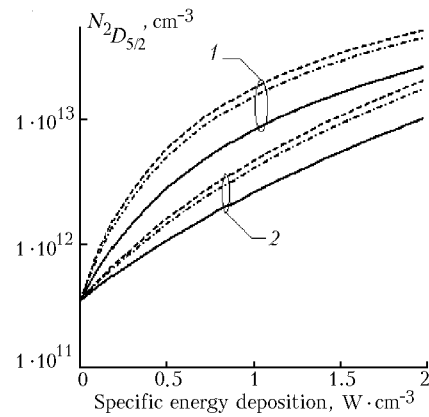


Fig. 3e. Balanced concentration of copper atoms in the D_{5/2} state with increasing energy deposition: cylindrical discharge channel (1), profiled discharge channel (2); energy deposition uniform over the cross section of the working channel (solid curve), triangular distribution of energy deposition (dashed curve), parabolic distribution of energy deposition (dot-and-dash curve).

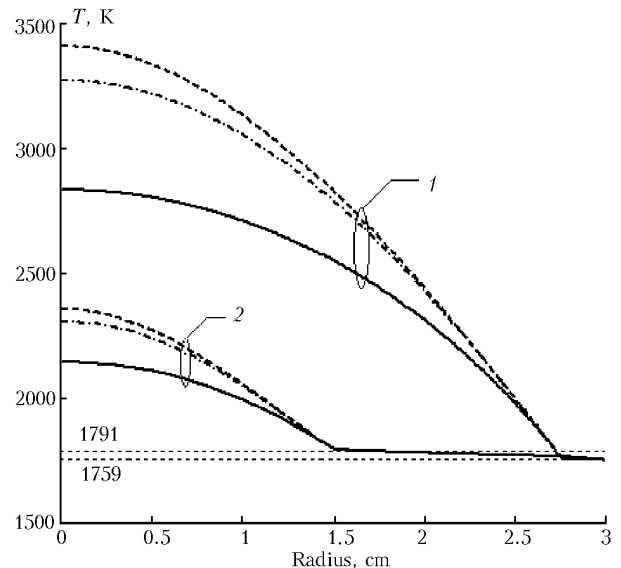


Fig. 4a. Gas temperature over the GDT radius at the specific energy deposition of 1 W/cm³: GDT of cylindrical geometry (1), GDT with profiled working channel (2); energy deposition uniform over the cross section of the working channel (solid curve), triangular distribution of energy deposition (dashed curve), parabolic distribution of energy deposition (dot-and-dash curve).

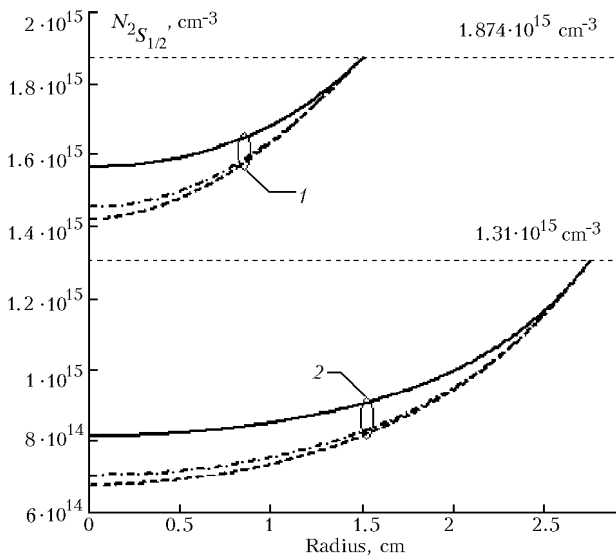


Fig. 4b. Distribution of the concentration of copper atoms in the ground state over the GDT radius at the specific energy deposition of 1 W/cm^3 : GDT with profiled working channel (1), GDT of cylindrical geometry (2); energy deposition uniform over the cross section of the working channel (solid curve), triangular distribution of energy deposition (dashed curve), parabolic distribution of energy deposition (dot-and-dash curve).

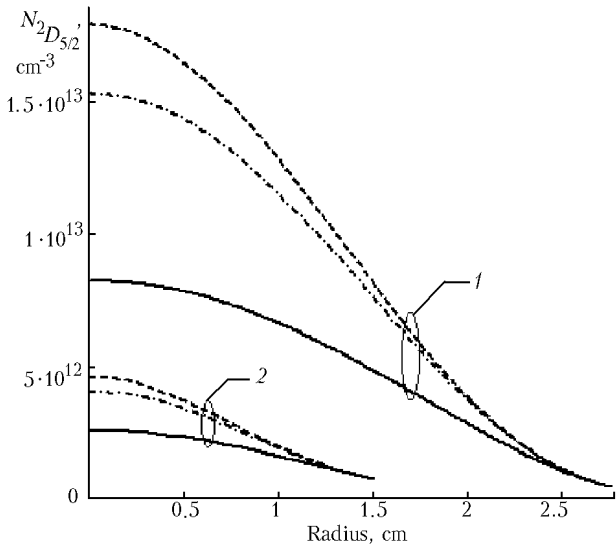


Fig. 4c. Radial distribution of the concentration of copper atoms in the $D_{5/2}$ state balanced with the gas temperature: GDT of cylindrical geometry (1), GDT with profiled working channel (2); energy deposition uniform over the cross section of the working channel (solid curve), triangular distribution of energy deposition (dashed curve), parabolic distribution of energy deposition (dot-and-dash curve).

The calculated results depicted in Fig. 4c illustrate the fact that for a GDT with the profiled discharge channel the level of population of copper atom metastable energy levels balanced with the gas temperature is far lower than that for the cylindrical

design of the discharge channel. Figure 4c depicts the radial distribution of the concentration of copper atoms in the metastable state. For GDT with the cylindrical geometry of the discharge channel, the ratio of the concentration of copper atoms in the metastable state on the axis to the concentration in the near-wall zone is equal to 19.901, while for GDT with the profiled discharge channel this ratio is only 3.677, that is, 5.412 times lower. This fact is indicative of the far higher degree of radial uniformity of the pre-pulse concentration of copper atoms in the metastable state, leading to higher uniformity of lasing and higher quality of the output radiation, which is the main advantage of gas lasers over solid-state lasers.

Effect of decrease of the diffusion length

Consider now the effect of variation of the diffusion length on the plasma parameters when radial inserts are introduced in the laser working channel. For the gas discharge tube of the cylindrical configuration, the diffusion length can be calculated as²⁷:

$$\frac{1}{\Lambda} = \sqrt{\left(\frac{2.405}{r}\right)^2 + \left(\frac{\pi}{L}\right)^2},$$

where r is the cylinder radius; L is the length of the cylindrical cavity. Since the second term is much smaller than the first one, especially in the case of the profiled working channel, the diffusion length is $\Lambda = r_p / 2.405$, where r_p is the average distance to the wall of the radial insert.

Thus, the use of a profiled working channel leads to a decrease in the diffusion length by more than order of magnitude, which significantly increases the role of diffusion processes. The diffusion energy efflux to the wall with following quenching of atoms in the metastable state and diffusion departure of electrons with the following recombination on the wall become more pronounced. Besides, the presence of the following term in the equation for description of the time dependence of the electron temperature:

$$-\frac{D_a(T_e)}{\Lambda^2} \frac{3}{2} k_B T_e,$$

where $D_a(T_e)$ is the coefficient of ambipolar electron diffusion, T_e is the electron temperature, and k_B is the Boltzmann constant, leads to a decrease of the electron temperature. This, in its turn, according to the equation $\frac{dN_e}{dt} = \gamma(T_e^{9/2}) N_e^3$, where γ is the coefficient of triple recombination, provides for more intense recombination of electrons in afterglow and, correspondingly, the decrease of the pre-pulse concentration of electrons.

Thus, the decrease of the diffusion length is one more factor explaining the effect of radial inserts on

the performance characteristics of a copper vapor laser. They are affected indirectly, through the decrease of the pre-pulse electron temperature and concentration (which agrees with Ref. 10), as well as the concentration of copper atoms in the metastable state.

Estimate the probability of nonuniform distribution of the electron temperature over the cross section of the GDT discharge channel by the end of the interpulse period in the laser. The analysis will be performed, following Refs. 28 and 29, by comparing the characteristic times of spatial relaxation of the electron temperature $\tau_e \cong \Lambda^2/D_e$, where D_e is the coefficient of electron diffusion³⁰; recombination heat release

$$\tau_{\text{rad}} \cong \frac{T_e}{J_{\text{Cu}} N_e^2 \beta},$$

where J_{Cu} is the copper atom ionization potential (7.726 eV); energy exchange with heavy particles (copper ions and neon atoms)

$$\tau_g \cong 2 \left(v_{\text{ei}} \frac{m_e}{M_i} + 2v_{\text{ea}} \frac{m_e}{M_a} \right)^{-1},$$

where m_e is the electron mass, M_i is the mass of copper ion, M_a is the mass of neon atom, v_{ei} is the frequency of Coulomb electron-ion collisions, v_{ea} is the frequency of electron-atom collisions. The effective frequency of Coulomb electron-ion collisions is³¹:

$$v_{\text{ei}} = \frac{4\sqrt{3}\pi e^4 N_e \ln \Lambda_C}{9 m_e^{1/2} T_e^{3/2}} \cong 5.076 \cdot 10^{-6} \frac{N_e \ln \Lambda_C}{\sqrt{T_e^3}},$$

where $\ln \Lambda_C$ is the Coulomb logarithm (≈ 10). The electron-atom frequency of collisions is calculated as³²:

$$v_{\text{ea}} = N_{\text{Ne}} \sqrt{3T_e/m_e} \sigma_{\text{tr}} \cong 1.089 \cdot 10^{-8} N_{\text{Ne}} \sqrt{T_e},$$

where N_{Ne} is the concentration of neon atoms; σ_{tr} is the transport cross section of electron scattering at a neon atom.

The calculations were performed for two "polar" values of the buffer gas pressure using the parameter values similar to those in Ref. 25: for pre-pulse values of the plasma parameters

1. $N_{\text{Ne}} = 1 \cdot 10^{17} \text{ cm}^{-3}$, $T_e = 0.302 \text{ eV}$, $N_e = 5 \cdot 10^{13} \text{ cm}^{-3}$;
2. $N_{\text{Ne}} = 1 \cdot 10^{16} \text{ cm}^{-3}$, $T_e = 0.216 \text{ eV}$, $N_e = 1 \cdot 10^{13} \text{ cm}^{-3}$.

At the concentration of neon atoms equal to $1 \cdot 10^{17} \text{ cm}^{-3}$

$$\tau_g = 1.154 \cdot 10^{-6} \text{ s}, \tau_e = 2.5 \cdot 10^{-6} \text{ s},$$

$$\tau_{\text{rad}} = 2.218 \cdot 10^{-5} \text{ s}, \text{ that is, } \tau_g < \tau_e < \tau_{\text{rad}}$$

and we can expect that the electron temperature is radially non-uniform for GDT of cylindrical geometry. However, for GDT with the profiled discharge channel $\tau_e = 2.5 \cdot 10^{-7} \text{ s}$ and the electron temperature is more uniform over the cross section of the discharge channel because the electron heat conductivity has time to follow the energy losses in collisions with heavy particles and recombination heating.

At $N_{\text{Ne}} = 1 \cdot 10^{16} \text{ cm}^{-3}$

$$\tau_g = 3.291 \cdot 10^{-6} \text{ s},$$

$$\tau_{\text{rad}} = 8.714 \cdot 10^{-5} \text{ s}, \text{ that is, } \tau_e < \tau_g < \tau_{\text{rad}},$$

therefore, the radial distribution of the electron temperature is uniform. The use of radial inserts allows achieving a uniform radial distribution of the electron temperature in the earlier periods of the interpulse gap, which provides for a uniform radial distribution of the electron concentration. This circumstance, along with more uniform distribution of the concentration of copper atoms in the ground state over the cross section of the discharge channel, leads to a more uniform radial distribution of copper atoms in the metastable state and, correspondingly, to more uniform lasing over the GDT cross section.

Conclusion

To clarify the mechanism of the effect of radial inserts in the working channel of a copper-vapor laser, the temperature field of the active element is calculated and variations of the diffusion length are analyzed. It is shown that the heat transfer in GDT with the profiled working channel allows a significantly higher power to be deposited to the laser active medium without its overheating as compared to GDT of cylindrical geometry. This occurs due to the weaker effect on lasing from such adverse phenomena as thermal deficit of metal atoms in the ground state on the axis of the working channel and thermal population of the copper atom metastable levels. Because of a decrease in the diffusion length and the increase in the degree of uniformity of the gas temperature, the use of radial inserts leads to a more uniform radial distribution of temperature and concentration of electrons, as well as copper atoms in the metastable state at the simultaneous decrease of the absolute values of these parameters. The calculated results are also indicative of the increase in the concentration of copper atoms in the working channel and better matching of the active element with the discharge circuit. In general, the calculations performed showed that the use of GDT with the profiled discharge channel should lead to improvement of energy and frequency characteristics, as well as the quality of the output radiation of a copper-vapor laser.

Thus, the known methods of improving the energy and frequency characteristics of copper vapor lasers by introducing active admixtures and copper compounds into the working channel can be complemented with design solutions, in particular, the use of specially profiled active elements.

References

1. A.N. Soldatov and V.I. Solomonov, *Gas Discharge Metal Vapor Self-Terminating Lasers* (Nauka, Novosibirsk, 1985), 152 pp.
2. V.M. Batenin, V.V. Buchanov, M.A. Kazaryan, I.I. Klimovskii, and E.I. Molodykh, *Atomic Metal Self-*

- Terminating Lasers* (Nauchnaya Kniga, Moscow, 1998), 544 pp.
3. N.A. Lyabin, A.D. Chursin, M.S. Domanov, *Izv. Vyssh. Uchebn. Zaved., Fizika* **42**, No. 8, 68–75 (1999).
 4. N.A. Lyabin, A.D. Chursin, S.A. Ugol'nikov, M.E. Koroleva, and M.A. Kazaryan, *Kvant. Elektron.* **31**, No. 3, 191–201 (2001).
 5. V.F. Fedorov and A.N. Soldatov, in: *Abstracts of Papers of the Siberian Meeting on Inverse Population and Lasing at Atomic and Molecular Transitions*, Tomsk, 1986, Part 1, p. 20.
 6. V.V. Vorob'ev, S.V. Kalinin, I.I. Klimovskii, I. Kostadinov, V.A. Krestov, V.N. Kubarev, and O. Marazov, *Kvant. Elektron.* **18**, No. 10, 1178–1180 (1991).
 7. N.V. Sabotinov, F. Akerboom, D.R. Jones, and C.E. Little, *IEEE J. Quantum Electron.* **31**, No. 4, 747–752 (1995).
 8. P.A. Bokhan, "Metal vapor lasers with collisional de-excitation of lower working layers," *Doct. Phys.-Math. Sci. Dissert.*, Tomsk–Novosibirsk (1988), 418 pp.
 9. D.R. Jones, A. Maitland, and C.E. Little, *IEEE J. Quantum Electron.* **30**, No. 10, 2385–2390 (1994).
 10. J.J. Chang, B.E. Warner, C.D. Boley, and E.P. Dragon, in: *Pulsed Metal Lasers*, ed. by C.E. Little and N.V. Sabotinov (1996), pp. 101–112.
 11. A.P. Soldatov, "Metal vapor self-terminating lasers with controllable lasing," *Doct. Phys.-Math. Sci. Dissert.* (Tomsk, 1998), 355 pp.
 12. A.N. Soldatov, Yu.P. Polunin, and L.N. Chausova, *Proc. SPIE* **2619**, 123–133 (1995).
 13. V.F. Fedorov, V.B. Sukhanov, G.S. Evtushenko, V.M. Pogrebenkov, and V.M. Klimkin, in: *Abstracts of Papers at XIII Symposium on Metal Vapor Lasers*, Lazarevskoe (2000), pp. 11–12.
 14. V.M. Batenin, I.I. Klimovskii, L.A. Selezneva, *Teplofiz. Vys. Temperatur* **18**, No. 4, 707–712 (1980).
 15. I.P. Zapesochnyi, V.A. Kel'man, I.I. Klimovskii, L.A. Selezneva, and V.Yu. Fuchko, *Teplofiz. Vys. Temperatur* **26**, No. 4, 671–680 (1988).
 16. G.S. Evtushenko and A.G. Filonov, *Atmos. Oceanic Opt.* **10**, No. 11, 824–826 (1997).
 17. V.N. Batygin, I.I. Metelkin, and A.M. Reshetnikov, *Vacuum-Dense Ceramics and Its Seals with Metals*, ed. by N.D. Devyatkov (Energiya, Moscow, 1973), 408 pp.
 18. V.L. Balkevich, *Technical Ceramics* (Stroiizdat, Moscow, 1984), 256 pp.
 19. *Basic Thermophysical Properties of Gases and Fluids* (Kemerovskoe Knizhnoe Izd., Kemerovo, 1971), 225 pp.
 20. I.I. Klimovskii, "Atomic metal self-terminating lasers," *Doct. Phys.-Math. Sci. Dissert.*, Moscow (1991), 467 pp.
 21. A.V. Elets'kii, Yu.K. Zemtsov, A.V. Rodin, and A.N. Starostin, *Transport Phenomenon in Plasma* (Atomizdat, Moscow, 1975), 220 pp.
 22. I.I. Novikov and K.D. Voskresenskii, *Applied Thermodynamics and Heat Transfer* (Atomizdat, Moscow, 1977), 352 pp.
 23. V. Isachenko, V. Osipova, and A. Sukomel, *Heat Transfer* (Mir Publishers, Moscow, 1974), 570 pp.
 24. A.V. Lykov, *Theory of Thermal Conductivity* (Vysshaya Shkola, Moscow, 1967), 600 pp.
 25. R.E. Honing, *RCA Review* **23**, No. 12, 567–586 (1962).
 26. R.J. Carman, *J. Appl. Phys.* **82**, No. 1, 71–83 (1997).
 27. E.W. McDaniel and E.A. Mason, *Mobility and Diffusion of Ions in Gases* (Wiley, New York, 1973).
 28. L.G. D'yachkov and G.A. Kobzev, *Zh. Tekh. Fiz.* **48**, No. 11, 2343–2346 (1978).
 29. V.M. Batenin, I.P. Zapesochnyi, V.A. Kel'man, I.I. Klimovskii, L.A. Selezneva, and V.Yu. Fuchko, "Radial inhomogeneities of plasma parameters in the period between pulses of self-heating copper vapor laser," Preprint No. 5-210, ICM AS, Moscow (1987), 32 pp.
 30. P. Baille, J.S. Chang, A. Claude, R.M. Gobson, G.L. Ogran, and A.W. You, *J. Phys. B.* **14**, 1485–1495 (1981).
 31. A.M. Boichenko, G.S. Evtushenko, O.V. Zhdaneev, and S.I. Yakovlenko, *Kvant. Elektron.* 2003 (in print).
 32. A.M. Boichenko, G.S. Evtushenko, S.I. Yakovlenko, O.V. Zhdaneev, *Laser Phys.* **11**, 580–588 (2001).